

THE DRIFT TUBE AND BEAM LINE QUADRUPOLE PERMANENT MAGNETS FOR THE NEN PROTON LINAC

R. F. Holsinger  
New England Nuclear Corp.  
N. Billerica, Mass. 01862

Summary

One hundred and nine permanent magnet quadrupoles of the new "Halbach type" will be installed in the drift tubes of the 45-MeV NEN proton linac. This new design concept utilizes, in a unique way, the anisotropy and other magnetic properties of oriented samarium-cobalt magnets to achieve high pole-tip fields and efficient use of the material. All of the drift tube quadrupoles have been designed, and the first group of 35 have been fabricated and measured. Prototype design work and computer modeling studies of similar large aperture permanent magnet quadrupoles, for the high energy beam transport system of the NEN linac, have been completed. These beam line quadrupoles will incorporate mechanisms by which their focusing strength may be adjusted.

Design Principles

Previous designs

The author and others<sup>1,2</sup> have been developing, for the past several years, permanent magnet quadrupoles for replacing electromagnets in applications such as the drift tubes in proton linacs. These previous designs were primarily based on replacing the coils in an electromagnet quadrupole with four suitably oriented pieces of samarium cobalt. The magnet on the right of Fig. 1 is a New England Nuclear prototype of such a "coil replacement" quadrupole. This square yoke quadrupole has an aperture radius of 1.3 cm and a pole-tip field of approximately 3.0 kilo-Gauss. These previous types of permanent magnet quadrupoles are limited to about 6 kilo-Gauss pole-tip fields using the best commercially available Rare Earth-Cobalt (REC) materials. The NEN linac requires quadrupoles with nearly 10 kilo-Gauss pole-tip fields in the low energy end of the Alvarez tank.

In the section below a new design principle will be briefly outlined, on which principle quadrupoles may be easily designed to provide pole tip fields of above 15 kilo-Gauss. This new design also makes very efficient use of the REC materials to produce medium and high strength gradient magnets.

Segmented ring quadrupoles

Recently, several papers by K. Halbach<sup>3,4</sup> and the author<sup>5</sup> have described the complete theory and some practical results of the new design principle. Selected results of this previous work will be reviewed here. It should be noted that a key spark for this new idea came from discovering the work of W. Neugebauer<sup>6</sup> on the clever use of the anisotropy of REC materials to minimize leakage flux in various permanent magnet assemblies.

J. P. Blewett<sup>7</sup> several years ago described a permanent magnet quadrupole created inside of a 4-pole symmetrically magnetized ring. He derived the relation for the pole tip field strength of such a quadrupole:

$$B_o = 2 \mu_o H_c \left(1 - \frac{r_i}{r_o}\right) \quad , \quad (1)$$

where  $r_i$  and  $r_o$  are the inside and outside radii of the ring,  $H_c$  is the H-coercive of the material, and it is assumed that the slope of the B-H curve is unity. With the  $H_c$  values of newer REC materials approaching 10 kilo-Oersted, such a quadrupole would lead to very strong pole-tip fields. The "missing link" in Blewett's work was provided by K. Halbach in his derivation of the required easy axis variation in anisotropic, oriented, permanent magnet material. The result is, referring to Fig. 2, that the easy axis direction in a magnetized ring must be varied as:

$$\alpha = 30 \quad (2)$$

Then, when the B-H function and the anisotropy are completely described by the relations:

$$\mu_o H_c = B_r \quad (3)$$

$$\frac{dB_{\parallel}}{\mu_o dH_{\parallel}} = 1, \mu_{\perp} = 1 \quad , \quad (4)$$

where  $B_r$  is the residual induction,  $\mu_{\parallel}$  and  $\mu_{\perp}$  are the parallel and perpendicular permeabilities relative to the easy axis, a magnet made with this "perfect" material produces an error-free quadrupole field. The strength of the pole-tip field in such a magnet is given by Eq. (1). Figure 2 is the flux plot of 1/8 of this type of quadrupole, calculated with the computer program PANDIRA.<sup>8</sup>

The practical solution to building a ring quadrupole with the easy axis directions prescribed by Eq. (2), is to divide the ring into a number of segments. The curved segments may be further approximated by trapezoids, and the resulting configuration for sixteen segments is shown schematically in Fig. 3. In this figure, the arrows inside of the trapezoids represent the easy axis directions, and the arrows on the dashed lines represent the directions of the quadrupole field. This sixteen-piece design has magnets with three different easy axis angles and five different easy axis orientations, counting polarity.

Number and shape of segments

The two most important theoretical parameters to consider when designing a segmented ring quadrupole are: 1) the decrease in the quadrupole strength due to the non-continuous easy axis orientation, and 2) the order and magnitude of the harmonic multipole field errors introduced by the geometrical shape effects of the pieces. For a segmented ring quadrupole with  $M$  trapezoidal pieces made of "perfect" REC material, the pole-tip field is given by:

$$B_o = 2\mu_o H_c \cos^2 \frac{\pi}{M} \frac{\sin \frac{2\pi}{M}}{\frac{2\pi}{M}} \left(1 - \frac{r_i}{r_o}\right) \quad . \quad (5)$$

For  $M = 16$ , Eq. (5) gives the result that the pole-tip field is reduced by only 6.3% compared to the continuous easy axis orientation.

The  $n$ th-order harmonic multipole error fields which are excited in a symmetrical array of  $M$  identically shaped (not necessarily trapezoidal) and rotationally symmetric pieces are:

$$n = 2 + kM; k = 1, 2, 3, \dots, (6)$$

i.e., for  $M = 16$  the first multipole error is  $n = 18$ , the 36-pole. The magnitude of the 36-pole for the specific case of 16 trapezoidal pieces with  $r_i/r_o = 1.1/3.0$  is 6.8% of the quadrupole field at 100% aperture, or 0.2% at 80% aperture. It has been pointed out by Halbach, that this error may be eliminated by a suitable thickness shim between the trapezoidal pieces, in which case the first theoretical error would be of order 34: the 68-pole.

#### Efficient use of the REC material

The ring quadrupole with the continuous easy axis orientation given by Eq. (2), obviously produces the strongest possible pole-tip field, as given by Eq. (1), for a specific  $r_i$ ,  $H_c$ , and volume of material. Such an arrangement makes very efficient use of the REC material. This can be understood qualitatively by examining the flux plot of 1/8 of an eight-piece segmented ring quadrupole, such as shown in Fig. 4. One can observe how the flux is guided into and concentrated in the aperture region. This is in contrast to the large amount of leakage flux lost into the sides of the poles of a conventional electromagnet quadrupole or permanent magnet quadrupole based on the "coil replacement" design principle. A way to appreciate quantitatively the efficient use of the REC material in the new design, is to note the fact that the material close to the aperture contributes a large fraction of the field strength. By comparison, quadrupoles based on the "coil replacement" design make inefficient use of the REC material placed at a significant distance from the aperture. For example, using Eq. (1) one finds that, in the new design, the material inside of the average radius  $r_a = (r_i + r_o)/2$  contributes 80% of the strength when  $r_i/r_o = 4$ , whereas this material comprises only 35% of the volume.

#### NEN Drift Tube Quadrupoles

#### Specifications and characteristics

The specifications of the 109 drift tube quadrupoles for the NEN linac are summarized in Table I. The quadrupoles are divided into three groups, each group with a different pole-tip field, aperture radius, and length, but all magnets have the same outside diameter.

Two characteristics of these new quadrupoles have important consequences for the NEN linac design. Since no space is required for a coil or cooling, the quadrupole can fill nearly the

entire length of the drift tube. This fact was used to advantage to achieve the required focusing strength,  $\int B' dz = B'_o l_{eff}$ , in the early drift tubes of the Alvarez tank. A unique property of the ring quadrupoles, which was derived by K. Halbach using symmetry arguments, is that the effective length,  $l_{eff}$ , is equal to the physical axial length of the permanent magnet assembly. The second characteristic of this new design, that was used to advantage, is that since the required focusing power could be achieved with quadrupoles of only 7 cm outside diameter, it was possible to design the linac focusing structure with drift tubes of 9 cm outside diameter rather than the conventional 18 cm diameter. This leads to significant savings in rf power, as well as having other advantages.<sup>9</sup>

#### Computer modeling and design

The mathematical modeling of REC magnet assemblies is greatly simplified if one assumes "perfect" material and no other saturable magnetic materials are present in the problem. In this case, an REC piece with a uniform and parallel easy axis orientation can be replaced by current sheets, or charge sheets, on each surface of the piece. The fields and multipole components produced by an array of charge sheets may then be calculated analytically, since the fields superimpose linearly. Reference 4, for example, gives a derivation of this computational method. Much of the original development of the segmented ring quadrupole was done using this computational model.

For analyzing problems with "non-perfect" permanent magnet materials and other saturable materials, the program PANDIRA has been used. PANDIRA solves anisotropic 2-D field problems with or without normal saturable magnetic materials and allows for very general boundary conditions and symmetries. Figure 5 shows the flux plot of 1/8 of a group I drift tube quadrupole, calculated with PANDIRA. The shape of the individual magnet pieces is a "modified trapezoid", where the sides of the pieces have been cut parallel towards the outside. This shape was designed to reduce the width of the pieces and accommodate a retainer spline which positions the pieces.

The computer analysis with PANDIRA gives the field quality in terms of harmonic multipole errors for a specified geometry and material characteristics. To investigate the accuracy of the program for these types of calculations and to determine the effects of "non-perfect" REC materials, a series of problems was solved; Table II gives the results of those calculations. In Table II, the "perfect" material has  $B_r = \mu_0 H_c = 8$  kilo-Gauss, and the "real" material has  $B_r = 8.7$  kilo-Gauss,  $H_c = 8.2$  kilo-Oersted and  $\mu_1 = 1.03$ .

The geometry of the magnet analyzed has  $r_i = 1.1$  cm,  $r_o = 3.0$  cm and the pieces are trapezoids in the first three columns and modified trapezoids in the last two columns, designated by "parallel". The "parallel" geometry is that of the group I drift

tube quadrupoles. The analysis shows that PANDIRA has an accuracy of about 0.2% for high order multipoles and that the "allowed" harmonic errors due to non-"perfect" material are less than about 0.5%.

#### Production and measurement of the SmCo<sub>5</sub> pieces

All of the magnet pieces for the NEN linac drift tube quadrupoles have been manufactured by Hitachi Magnetics Corp., Edmore, Michigan. The material designation is Hicorex 90B, a SmCo<sub>5</sub> compound which has nominal properties of  $B_r = 8.7$  kilo-Gauss,  $H_c = 8.2$  kilo-Oersteds,  $H_{ci} > 15$  kilo-Oersteds, where  $H_{ci}$  is the intrinsic coercivity, and a recoil permeability of 1.05.

The magnet pieces for the group I and group II drift tube quadrupoles were manufactured in the following steps. First, a block of the SmCo<sub>5</sub> material was magnetically aligned and pressed, and then sintered. This block, with approximate dimensions of 2 by 2 by 1/2 inches, has the easy axis angle aligned parallel to a 2-inch dimension, and the pressing direction is parallel to the 1/2-inch dimension. At present, this block is the largest piece of SmCo<sub>5</sub> being manufactured in large quantity. Modified trapezoidal shaped pieces are then cut out of this block, with the cutting directions parallel, perpendicular and at 45° to the easy axis orientation, so as to provide the three easy axis angles. Next, the pieces are finish ground to the required dimensions and then given a further heat treatment to enhance the coercivity. Finally, the pieces are magnetized in an external field of the specified polarity. The manufacture of the group III magnet pieces differs from the above procedure in that individual blocks are made for each piece in the pressing, easy axis alignment, and sintering stage. In this case, the three easy axis angles are provided by rotating the die relative to the alignment magnetic field.

The final stage of manufacture is to measure the effective magnetic dipole moment per unit volume of each piece and record this along with the serial number. To verify the manufacturer's data, this measurement is made at NEN with an apparatus, as shown in Fig. 6, consisting of a Helmholtz coil pair with a mechanism for positioning and rotating the pieces in the center of the coil pair, and an integrating voltmeter connected to the coils. A magnet piece is inserted in the positioning mechanism with its easy axes parallel to the axis of the coil system, the integrator is zeroed, and then the piece is quickly rotated by 180°. The integrated induced voltage in the coil pair is proportional to the dipole strength of the piece.

This measurement also includes the effect of misalignment of the easy axis angle, since the integrated signal is also proportional to the alignment of the dipole axis with the coil axis. It would be possible to measure the easy axis angle alignment relative to the axis of the piece with this apparatus, using a modified procedure.

The significance of this data is that it provides a measure of the variation of the "strength" of

the pieces due to manufacturing variables. This information gives essentially one point (open magnetic circuit) on the B-H curve, averaged over the piece. Figure 7 shows a typical distribution of magnet piece "strength" for one particular easy axis orientation.

#### Assembly procedure

The critical practical aspect of building permanent magnet quadrupoles is to minimize the low order harmonic errors, especially the  $n = 3$  sextupole error. In contrast to electromagnet quadrupoles, where it is simple to provide equal excitation of each pole, the permanent magnet material variables are difficult to control and somewhat tedious to measure. Fortunately, two characteristics of the new design make it possible to reduce the  $n = 3$  multipole error to a very small value.

The first step in the assembly procedure, aimed at producing high precision quadrupoles, is to select well matched pieces in terms of "strength" for each magnet assembly. This will help assure the equal "excitation" of each pole. The dipole strength per unit volume data for all the approximately 1800 pieces for the group I drift tube quadrupoles is entered into a data base on a digital computer system. A program was written which examines this data base and makes the selection of the 48 pieces which are the best matched in strength for a particular magnet assembly.

The actual putting together of 48 magnetized SmCo<sub>5</sub> pieces into a nearly zero-clearance close-packed assembly presents a real challenge. The minimum clearance between the pieces themselves and the pieces and the aluminum retainer spline is achieved by determining the maximum thickness of brass shim strips to fit between the outer end of the pieces and the slots in the spline. The photograph in Fig. 8 shows the assembly fixture which is used to clamp and position the pieces during assembly.

Since each group I quadrupole assembly consists of three layers and the multipole fields from each layer superimpose almost exactly linearly, it is possible to rotate two layers by 180° with respect to one fixed layer and in this way minimize the axially integrated  $n = 3$  error in the quadrupole. To this end, each quadrupole is measured after one layer is in place, and then again after two layers, and finally the complete assembly. From these three measurements, the phase and amplitude of the  $n = 3$  error in each layer may be inferred. If the  $n = 3$  error in the complete magnet assembly is larger than acceptable, one or two layers are rotated by 180° so that the superimposed sextupole fields approximately cancel each other. With this procedure, it has been possible to set the allowable limit of the  $n = 3$  error at 0.3% of the quadrupole field at 100% aperture radius.

#### Harmonic multipole measurement

Usually the field quality in a multipole magnet is described in terms of the strength and phase of the harmonic multipole errors relative to the fundamental desired field distribution at the

magnet aperture. An elegant and simple mathematical description of superimposed multipole fields in two dimensions can be made using the concept of the complex potential. These ideas and formulae will be briefly reviewed here. The complex potential inside the aperture of a multipole magnet is written as

$$F(z) = \sum_n C_n \left(\frac{z}{r_i}\right)^n = A(x,y) + iV(x,y) , \quad (7)$$

where  $z$  is the complex space variable  $x + iy$ , and the distances are normalized by  $r_i$ , the aperture radius of the magnet.

The  $C_n$ 's in this equation are the complex coefficients for the potential of the superimposed multipoles ( $n = 2$  is the quadrupole component), and  $A$  and  $V$  are the real (vector) and imaginary (scalar) parts of the complex potential. It can be shown that the magnetic field is related to the complex potential through the following equation:

$$\frac{B_x - iB_y}{y} = iF'(z) = i\sum_n \frac{C_n}{r_i^n} \left(\frac{z}{r_i}\right)^{n-1} . \quad (8)$$

The strength and phase of each multipole field component is given by the coefficient  $nC_n/r_i = B_n$  in this equation.

Equipment for measuring the multipole field components in small aperture quadrupoles was designed and built at NEN. Reference 5 gives a detailed description of this equipment. Precision measurements of the multipole errors in the quadrupole are made by slowly rotating a coil coaxial with the magnet and recording the induced voltage at 128 steps in one revolution. The coil is long compared to the axial length of the magnet and, therefore, measures the axial integral of flux distribution, including the fringe fields, which is equivalent to the vector potential  $A(\phi)$  in the 2-D case. This integrated signal is Fourier analyzed to yield the phase and amplitude of each harmonic multipole, i.e., the  $B_n$ 's, up to  $n = 18$ , the 36-pole.

The right hand column of Table II gives the results of the harmonic multipole measurements of the group I drift tube quadrupoles. The values in this table are averages for the approximately 35 magnets that have been assembled. The "allowed" harmonic errors  $n = 6, 10$  and  $14$  are primarily due to "non-perfect" material properties plus imperfect matching between magnet types, and the  $n = 18$  is inherent in this segmented ring quadrupole design. The small remaining "non-allowed" harmonic errors are attributed to a combination of three factors: 1) mechanical tolerances, 2) errors in easy axis orientation, and 3) variation in the B-H properties from the ideal straight line, which is particularly probable in the third quadrant of the B-H curve.

### Large Aperture Beam Line Quadrupoles

#### Design study

If the obvious advantages of permanent magnet quadrupoles can be utilized in large aperture beam line magnets, significant economies and simplifications of such systems would result. The two main problems to be solved are 1) making the quadrupole focusing strength adjustable, and 2) controlling the total cost of the quadrupole assembly to keep it comparable to that of an electromagnet, including the power supply.

Towards controlling the cost of the REC pieces, it is important to simplify the shape of the pieces and relax the tolerances to reduce the machining costs. Only a small fraction of the cost of the magnet pieces for the drift tube quadrupoles is due to raw material expense. Probably the least expensive shape to produce is one with a rectangular cross section.

Figure 9 shows the flux plot of 1/8 of the prototype design for a NEN beamline quadrupole. The aperture diameter of this quadrupole is 3.1 inches and the REC pieces have a cross-section of 1 by  $\frac{1}{2}$  inches. The PANDIRA analysis of this configuration with Hicorex 90B material, gives a pole-tip field of 4.3 kilo-Gauss. The REC pieces in this design are separated by small gaps at the aperture, which will allow the use of an external spline to position the pieces, rather than the combination internal spline and modified trapezoidal shaped pieces as in the drift tube quadrupole design. This will significantly reduce the tolerances on the pieces and still allow for the positioning accuracy required to produce precision quadrupole fields. Although the gaps between the pieces create a larger  $n = 18$  harmonic error than in the close-packed drift tube quadrupole design, the error is only 0.1% of the quadrupole field at 75% aperture, which is quite acceptable for our beamline magnets.

Several different schemes have been proposed for adjusting the focusing strength of permanent magnet quadrupoles.<sup>4,5</sup> The most obvious way is to add or subtract layers, which is quite feasible due to the modular construction. For continuous adjustment, the most practical arrangement is one that consists of several axial layers which are rotated with respect to each other to provide the adjustability. Figure 10 illustrates a four-layer assembly in which successive layers have been rotated alternately by  $\pm 22\frac{1}{2}^\circ$ . Since each layer produces a quadrupole field and the fields from each layer superimpose linearly, the axial integral is a quadrupole field with a reduced strength proportional to the cosine of twice the rotation angle. The mechanical design of such a quadrupole requires that the magnet pieces in each layer be clamped independently and that bearings be provided for precise radial and

axial alignment during the rotation. The axial force between the layers must also be supported. This force changes from maximum repulsion to maximum attraction during a  $\pm 45^\circ$  rotation of two layers.

#### Beam dynamics considerations

The multilayer adjustable quadrupole may be analyzed, from the beam dynamics point of view, as a series of short adjacent quadrupoles, rotated from the principle x and y focusing planes. Such a configuration leads to x-y coupling terms in the transfer matrices and some preliminary work has been done to investigate the significance of these effects. One promising configuration that has been analyzed consists of four 1/2" long layers, where the first and last layers are rotated by a positive angle and the middle two layers are rotated by the same angle in the opposite direction. For example, consider the case where this rotation angle is chosen to be  $20^\circ$ , which gives a 23% reduction in the integrated quadrupole strength. For this quadrupole, the emittance growth has been evaluated for a typical beam and found to be less than 1%. An investigation is underway<sup>10</sup> which may allow the elimination of x-y coupling in a multilayer adjustable quadrupole. This scheme would use the ratios and values of the rotation angles of some number of layers as free parameters with which to minimize or eliminate the coupling terms.

Multilayer adjustable quadrupoles will be incorporated in the high energy beam transport system of the NEN proton linac. These quadrupoles will have the following approximate specifications: an aperture diameter of 4 inches, a pole-tip field of 3 kilo-Gauss, an effective length of 2 to 8 inches. These elements will be arranged in triplet configurations.

#### Acknowledgements

K. Halbach provided inspiration and guidance in most aspects of the work described here. R. L. Gluckstern has contributed significantly to the multilayer adjustable quadrupole ideas and D. Comastras has helped in discussions and analysis on this problem. The work of N. E. Webber in computer programming and analysis and W. Polewarczyk in skillfully assembling and measuring the drift tube quadrupoles is greatly appreciated. Thanks also goes to W. E. Jule and I. Gruverman for their enthusiastic support of this work.

#### References

1. B. P. Murin, V. I. Rogachev, and A. P. Fedotov, "Concerning the Possibility of using Quadrupoles with Permanent Magnets in Linear High-Energy Proton Accelerators", *Inst. Exp. Tech.*, 19(2), (1976).
2. N. Saito, E. D. Bush, and D. A. Swenson, "Development of Samarium-Cobalt Quadrupole Lenses for Particle Accelerator Applications", *Proceedings of the Third International Workshop on Rare Earth-Cobalt Permanent Magnets and their Applications*, (1978).

3. K. Halbach, "Strong Rare Earth Cobalt Quadrupoles", *IEEE Trans. Nucl. Sci.*, NS-26, 3882 (1979).
4. K. Halbach, "Design of Permanent Multipole Magnets with Oriented Rare Earth Cobalt Material", *Nuclear Instruments and Methods*, to be published.
5. R. F. Holsinger and K. Halbach, "A New Generation of Samarium-Cobalt Quadrupole Magnets for Particle Beam Focusing Applications", *Proceedings of the Fourth International Workshop on Rare Earth Cobalt Permanent Magnets and their Application*, (1979).
6. W. Neugebauer, "Low Flux Leakage Magnet Construction", U. S. Patent No. 3,768,054, Oct. 23, 1973.
7. J. P. Blewett, BNL Internal Report AADD-89, unpublished, (1965).
8. K. Halbach, R. F. Holsinger, to be published.
9. D. Comastras, "Accelerating Structure Parameters of the New England Nuclear Corp. Proton Linac", (Proceedings of this conference).
10. R. L. Gluckstern, private communication.

|                             | APERTURE<br>RADIUS<br>(CM) | POLE-TIP<br>FIELD<br>(K Gauss) | GRADIENT<br>(K Gauss/cm) | MAGNET LENGTH<br>• L <sub>EFF</sub><br>(CM) | OUTSIDE DIA<br>(CM) |
|-----------------------------|----------------------------|--------------------------------|--------------------------|---|---------------------|
| GROUP I<br>D.T. 0 to 27     | 1.10                       | 9.6                            | 8.7                      | 3.81  | 6.95                |
| GROUP II<br>D.T. 28 to 70   | 1.35                       | 8.1                            | 6.0                      | 5.08  | 6.95                |
| GROUP III<br>D.T. 71 to 108 | 1.60                       | 5.7                            | 3.6                      | 7.62  | 6.95                |

#### NEN LINAC DRIFT TUBE QUADRUPOLE PARAMETERS

Table I

| n          | Charge<br>Sheet<br>"Perfect" | PANDIRA<br>"Perfect" | PANDIRA<br>"Real" | PANDIRA<br>"Real"<br>Parallel | Measured<br>H-90B<br>Parallel |
|------------|------------------------------|----------------------|-------------------|-------------------------------|-------------------------------|
| 2 gauss    | 9500.                        | 9500.                | 10020.            | 9550.                         | 9609.                         |
| 3 (% of 2) |                              |                      |                   |                               | 0.21%                         |
| 4          |                              |                      |                   |                               | 0.33                          |
| 5          |                              |                      |                   |                               | 0.30                          |
| 6          | -                            | 0.0                  | 0.5               | 0.4                           | 0.25                          |
| 7          |                              |                      |                   |                               | 0.20                          |
| 8          |                              |                      |                   |                               | 0.26                          |
| 9          |                              |                      |                   |                               | 0.23                          |
| 10         | -                            | 0.0                  | 0.0               | 0.0                           | 0.56                          |
| 11         |                              |                      |                   |                               | 0.14                          |
| 12         |                              |                      |                   |                               | 0.13                          |
| 13         |                              |                      |                   |                               | 0.10                          |
| 14         | -                            | 0.2                  | 0.5               | 0.5                           | 0.15                          |
| 15         |                              |                      |                   |                               | 0.21                          |
| 16         |                              |                      |                   |                               | 0.09                          |
| 17         |                              |                      |                   |                               | 0.31                          |
| 18         | 6.8                          | 6.8                  | 6.8               | 6.9                           | 6.20                          |

Calculated and Measured Multipoles at 100% Aperture Radius

Table II

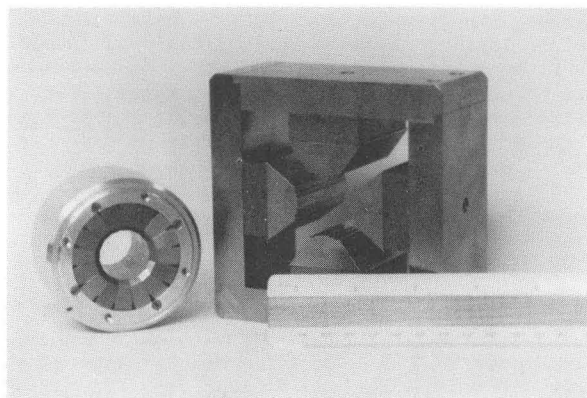
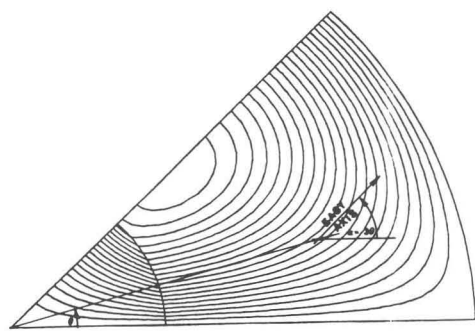
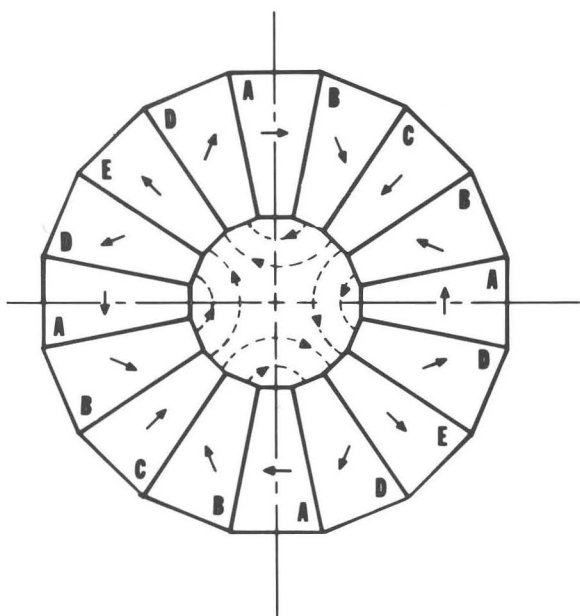


Fig. 1



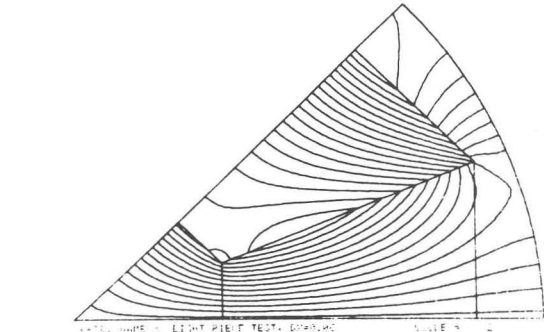
Flux Plot of "Perfect" REC Quadrupole

Fig. 2



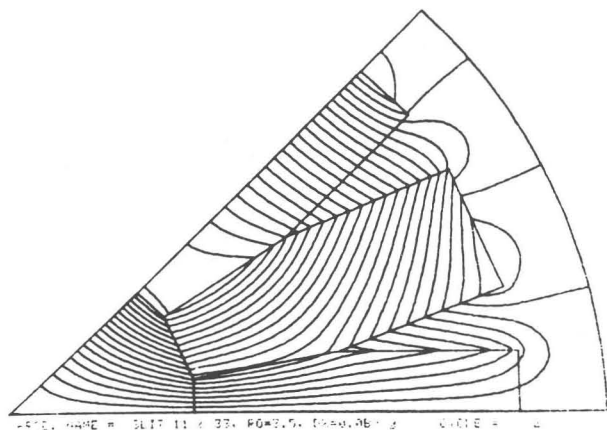
Schematic of 16 Piece Segmented REC Quadrupole With 5 Easy Axis Orientations

Fig. 3



Flux Plot of 8 Piece Segmented REC Quadrupole

Fig. 4



Flux Plot of 16 Piece Segmented REC Quadrupole With 5 Easy Axis Orientations

Fig. 5

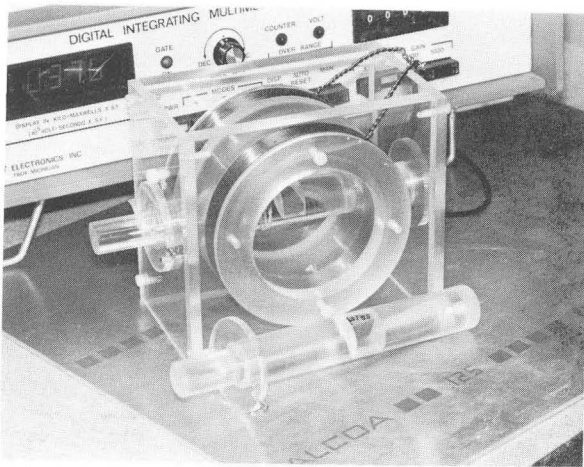


Fig. 6

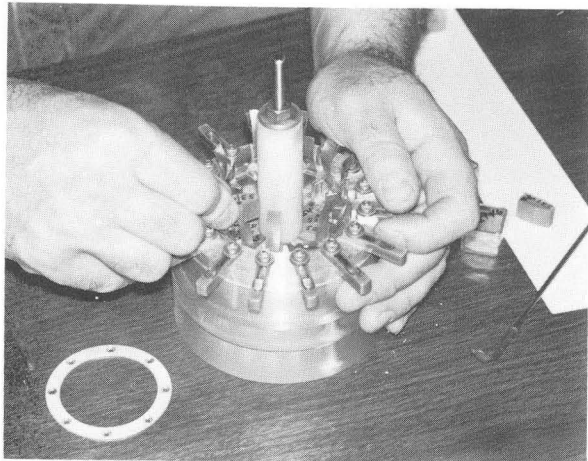
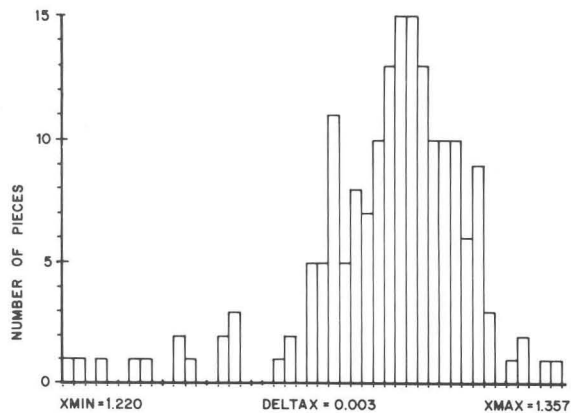
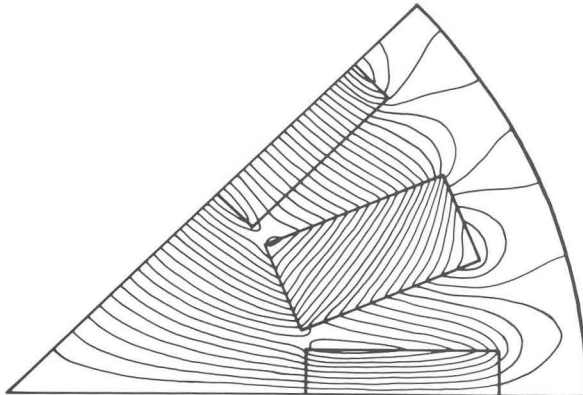


Fig. 8



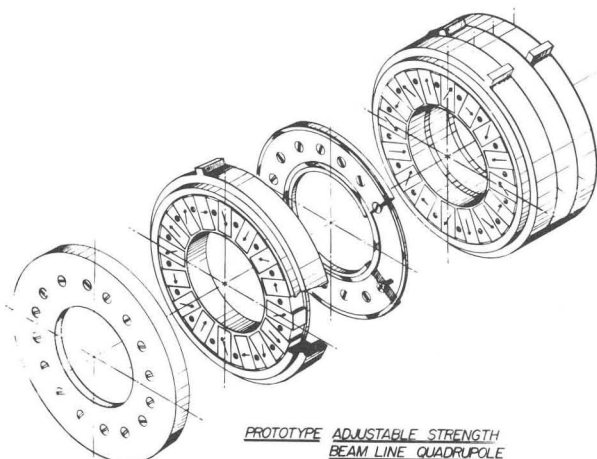
### TYPICAL DISTRIBUTION OF MAGNET PIECE DIPOLE STRENGTH

Fig. 7



## FLUX PLOT OF PROTOTYPE ADJUSTABLE STRENGTH QUADRUPOLE

Fig. 9



PROTOTYPE ADJUSTABLE STRENGTH  
BEAM LINE QUADRUPOLE

Fig. 10